*Journal of Directed Energy*, **3**, Winter 2009, 239–256

# Ablative Polymeric Materials for Near-Infrared High-Energy Laser Beam Diagnostics

**Christopher T. Lloyd,* Robert F. Cozzens, and Collin J. Bright**
*Naval Research Laboratory, 4555 Overlook Avenue, SE, Washington, D.C. 20375*

**and**

**D. Jason (Jake) Sames, Larry K. Myers, and Peter D. Kazunas**
*The Electro-Optics Center, 222 Northpointe Boulevard, Freeport, Pennsylvania 16229*

*One-micron lasers are of high interest for industrial and military applications fueled by recent developments in fiber lasers. There exists a large gap in data collection for the ablation of polymeric materials with near-infrared (IR) lasers. It is necessary to understand how and why chemical structural properties such as aromaticity, heteroatomic content, and degree of cross-linking affect near-IR ablation of polymers, as well as thermal stability and optical properties. More so, properties such as these are useful for determining which polymers are best suited for laser beam diagnostic measurements. Polymers such as clear Plexiglas® have been used as beam diagnostic materials at 10.6 μm in the past. Identification of two commercial polymers was made for laser beam profiling and diagnostic purposes at near-IR wavelengths. Differences in ablation and beam diagnostics using carbon black–loaded plastics were observed. Several synthesized and commercial polymeric materials were irradiated with a 10-kW, 1.07-μm fiber laser, and corresponding ablation energies were obtained. Ablation energies are dependent on the molecular structure of polymers, especially aromatic and heteroatomic character and thermal degradation processes. This study was aimed at understanding how near-IR radiation ablates polymers and to evaluate different polymers for use as potential irradiance diagnostic tools (witness plates).*

**KEYWORDS:** Carbon black, HEL irradiation, Irradiance diagnostics, 1.07-μm fiber laser, Polymer ablation

## 1. Introduction

Fiber lasers have become of interest for industrial and military applications due to reduced space requirements and lack of complex optics for beam routing. Material interactions with near-infrared (IR) fiber lasers have not been thoroughly studied. Much of the past work dealing with laser ablation of polymers has been performed using ultraviolet (UV)[1–4,7,8,12,14–17] or IR[5,6,9–11,13] lasers. A number of naturally colored polymers were used in these studies, as most organic polymers absorb strongly in these regions. However, at near-IR

Received March 10, 2009; revision received June 5, 2009.
*Corresponding author; e-mail: chris.lloyd@navy.mil.

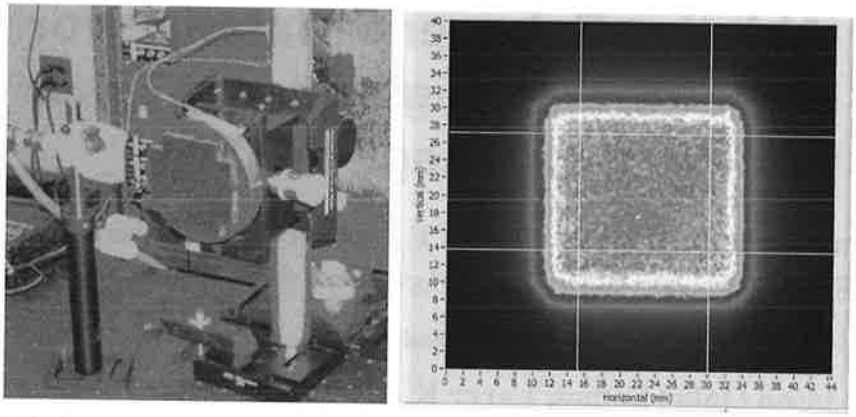

**Fig. 1.** Left: The segmented mirror used to create a uniform, square beam shape. Right: Digital image of the laser profile and ROI used to calculate the average irradiance on target.

wavelengths, ablation of polymeric materials requires pigments or fillers such as carbon black to increase absorptivity. Near-IR interactions with organic polymeric materials can be quite different. Whereas industry has obvious vested interests in polymer ablation in the near-IR, military applications involve using polymeric materials for high-energy laser (HEL) beam profiling and diagnostics. Beam diagnostics have been performed in the past with $CO_2$ lasers using clear Plexiglas®. Owing to the lack of absorption of clear Plexiglas® at near-IR wavelengths, alternative polymeric materials with appropriate pigments are employed for HEL beam profiling. The main focus of this study was not to investigate industrial or military–relevant materials but rather to narrow the list of useful beam profiling materials that will aid in future HEL–near-IR tests. The result is a better understanding of near-IR laser interactions with polymeric materials and corresponding ablation energies.

## 2. Experimental Laser Configuration

Tests were performed by the Electro-Optics Center/Pennsylvania State University (EOC) in Freeport, Pennsylvania. An IPG Photonics 10-kW Nd:YAG fiber laser was used for coupon testing. The laser combines 18 single-mode modules (17 active, 1 spare) into a single 100-$\mu$m output. Each module was nominally 600 W to sum to >10-kW output. Laser wavelength was 1.07 $\mu$m with a 3-dB bandwidth of approximately 3 nm. The beam parameter product (BPP) was measured by IPG to be 4 mm·mrad. The laser and chiller platform together occupy a footprint of approximately 1.2 and 1.5 $m^2$, respectively. The 20-m-long output fiber was terminated with a 12.4-cm Precitec collimator (COL YW50 125 QBH). A segmented mirror with reimaging optics created the desired, uniform profile. The mirror, which produced the square profile, was chosen to afford a highly uniform irradiance profile. The segmented optic and a sample beam profile are shown in Fig. 1. Typically, a "region-of-interest," or ROI, was defined on the profile where the average irradiance was calculated and reported. Once the ROI was defined, the required laser power could provide a desired irradiance. Beam spot size was kept constant at 6.5 $cm^2$, and power was varied to provide average irradiances from 250 to 1,000 $W/cm^2$.

The laser laboratory configuration is shown in Fig. 2. Ablation videos were recorded using a Norpix Basler monochromic camera at 60 frames per second with a 640 × 480 resolution. StreamPix software was used to trigger the camera and record burn through

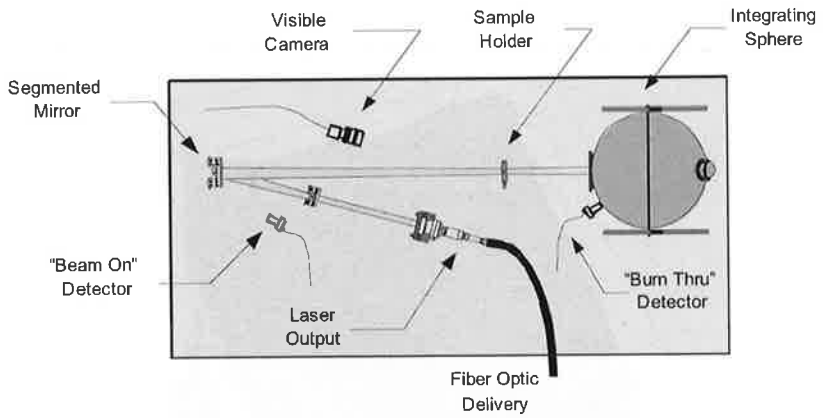


**Fig. 2.** Schematic of laser laboratory configuration used for polymer sample testing.

times. High-speed photodetectors (Thorlabs PDA400) were used for burn through time measurements. A "beam on" detector aimed at the segmented optic picked up scattered light and indicated precisely when the laser beam was on. Behind the target, a large, 51-cm-diameter integrating sphere captured divergent rays that broke through the sample. The second photodetector connected to the integrating sphere precisely signaled burn through. Time difference between the two detectors provided the burn through time. An exhaust hose located to the right of the sample holder (not shown) generated a clearing airflow for removal of any smoke or debris formed during irradiation.

Peak irradiance was determined using a Primes laser beam analyzer, which collected individual irradiance values per pixel over the beam spot (6.5 $cm^2$). The irradiance around the area of highest intensity was averaged and designated as the peak irradiance. Peak irradiance was used in calculations rather than average irradiance because most polymers have low thermal conductivity. A graph of the irradiance profile can be seen in Fig. 3.

## 3. Polymeric Materials Selection

Many of the black plastics or carbon-loaded polymeric materials used in this study were commercially available and acquired through several different manufacturers and/or their respective distributors. Generally, 0.64-cm-thick either 39- or 77-$cm^2$ sheets of material were ordered. From Piedmont Plastics (Beltsville, Maryland), high-density polyethylene (HDPE) and Acrylite GP were acquired. Acrylite GP and FF were manufactured and supplied by Evonik Cyro LLC. Polycarbonate (PC), Nylon 6,6, and the Kydex® sheet materials were supplied by Polymer Plastics (Reno, Nevada). Kydex® was manufactured by Kleerdex Company (Bloomsburg, Pennsylvania). Ultra-high-molecular-weight polyethylene (UHMW-PE) and Delrin® 150 (manufactured by DuPont) were all obtained through McMaster–Carr in Robbinsville, New Jersey. All materials were cut to size (13 $cm^2$) before laser testing using a band saw.

Poly(methyl methacrylate) (PMMA) samples were synthesized in our laboratory and cross-linked with various concentrations of ethylene glycol dimethacrylate (EGDMA). Concentrations of cross-linking agent added ranged from 1% to 35% by weight. All synthesized polymers were pigmented with carbon black in the form of a paste, E80-B, which was purchased from Aerospace Composites Products.

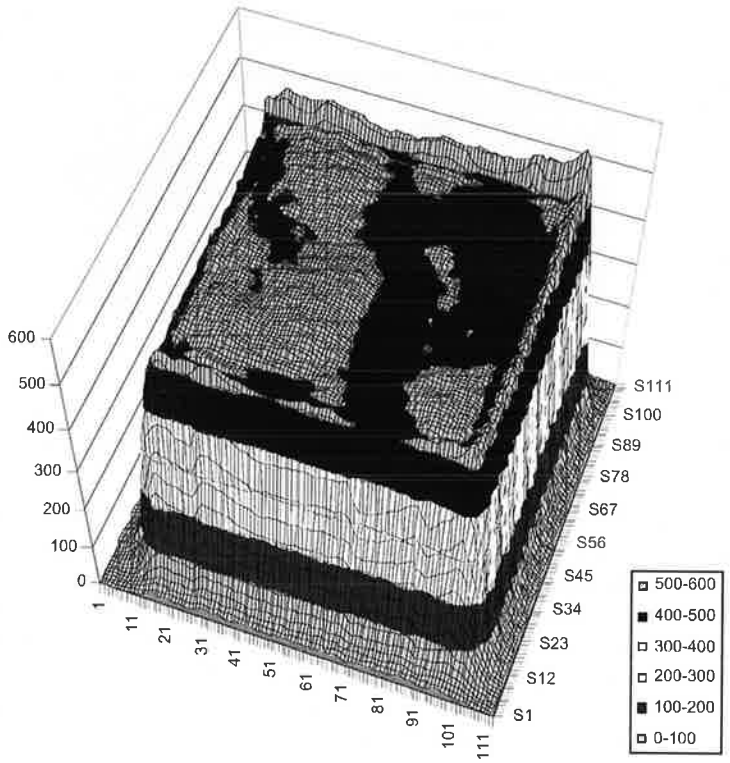


**Fig. 3.** Beam profile (6.5 $cm^2$) of 1.07-$\mu$m Nd:YAG fiber laser used for polymer ablation tests. Note the large peak irradiance area in the lower left-hand corner of the profile. Irradiance in watts per square centimeter is plotted on the $z$ axis; the $x$ axis and $y$ axis are positional coordinates.

## 4. Polymer Ablation Results

### 4.1. Ablation of cross-linked PMMA

Several series of laser tests at 1.07 $\mu$m were conducted on PMMA substrates as well as other polymers. Ablation energies were calculated upon irradiation of 0%–35% (0–0.005 $mol/cm^3$) cross-link agent–added PMMA samples; the results are shown in Fig. 4. Peak irradiance was 508 $W/cm^2$. Each data point in Fig. 4 represents the average ablation energy of several runs at a given cross-link density. The error associated with each data set was low, other than those of the 5% and 35% added samples, where the error was ~15% and 60%, respectively.

Although some randomness was observed in the ablation of PMMA samples with lesser amounts of cross-linking, average ablation energy was ~2.5 $kJ/cm^3$. It was expected that ablation energy would be lower for un-cross-linked PMMA than for cross-linked PMMA, yet this was not the case. Cross-linked polymers generally tend to have higher thermal stability than those not cross-linked due to polymer networking. At 5% cross-linking agent added, the data were somewhat erratic. This scatter could be a result of inhomogeneity of cross-linking in the sample. As the percentage of cross-linking was increased, ablation

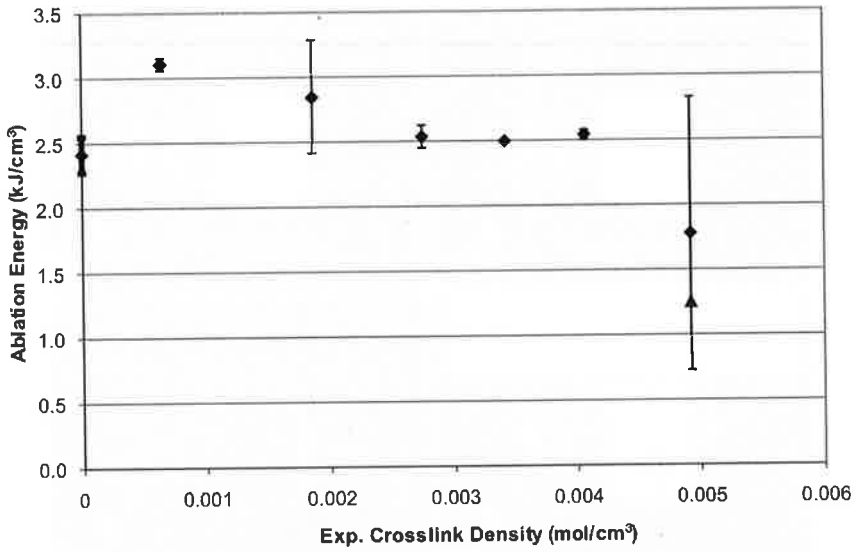


**Fig. 4.** Average ablation energy measured as a function of experimental cross-link density for PMMA using a 1.07-$\mu$m Nd:YAG fiber laser.

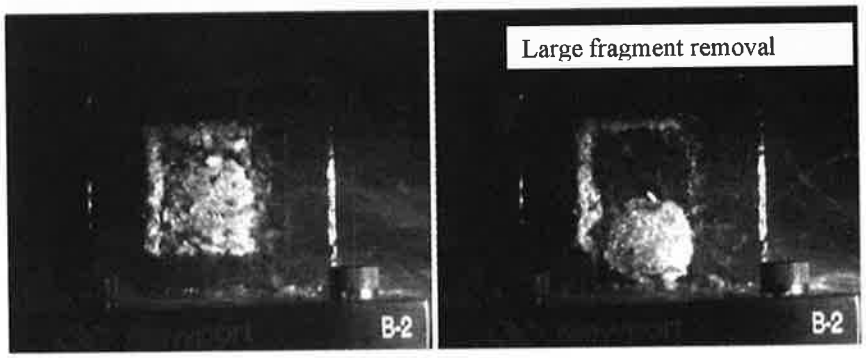


**Fig. 5.** Video clips of removal of large piece of 35% added cross-linking agent PMMA, resulting in low ablation energy.

energy was expected to gradually increase, but again this was not observed. Fragmentation of polymer chains likely played a large role. If large fragments of molecules were removed during ablation, less energy would be required to penetrate the sample. At a lower percentage of cross-linking, monomer vapor is formed by a more uniform degradation process.

With the 35% added cross-linking agent PMMA sample, the average ablation energy decreased to $\sim$1.8 kJ/cm$^3$, which was not expected. The outlying data point at 35% was due to the loss of a large fragment of material during irradiation, which lowered the ablation energy dramatically, and thus a large error was observed. Viewing the penetration video justified that conclusion. Just before penetration, the structural integrity of the sample was weakened and a large chunk of solid material was removed (Fig. 5).

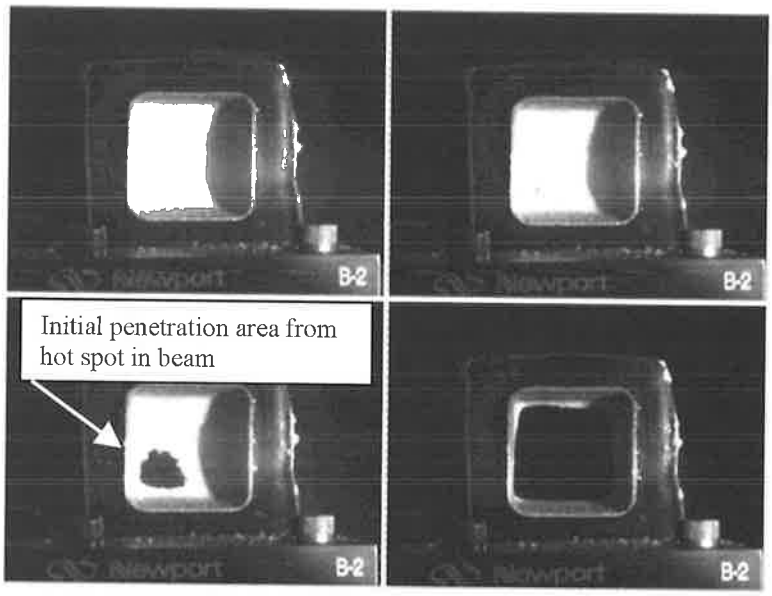


**Fig. 6.** Video clips of the ablation of a 1% added cross-linking agent PMMA sample.

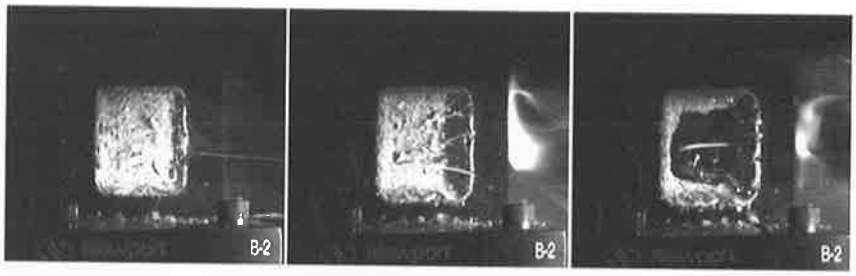


**Fig. 7.** Video clips of the ablation of a 25% added cross-linking agent PMMA sample.

After observing the large volume of material ablated from the 35% added cross-linked sample, we compared the video observations of the low-end cross-linked samples to the high-end cross-linked samples. In doing so, several conclusions were drawn. As mentioned above, the "hot" region as shown in the beam profile was in the lower left-hand corner of the spot; upon viewing the video frame by frame, in each case penetration was first observed in the lower left-hand region of the samples, which correlated well with the beam profile measurement (see Fig. 3).

Figures 6 and 7 clearly show the difference. As shown in the real-time video clips of Fig. 6, a 1% added cross-linking agent PMMA sample, when irradiated, cleanly ablated with no obvious fragments of material removed. The polymer depolymerized, or unzipped, affording monomer vapor. The resulting pattern ablated in the sample was smooth with no build-up of material around the edges. Figure 7 shows real-time ablation video clips of a 25% added cross-linking agent PMMA sample, in which material fragmentation and bubble formation is obvious. The ablated surface was rough, and residue was deposited at the cooler edges. This observed fragmentation was likely due to removal of the large

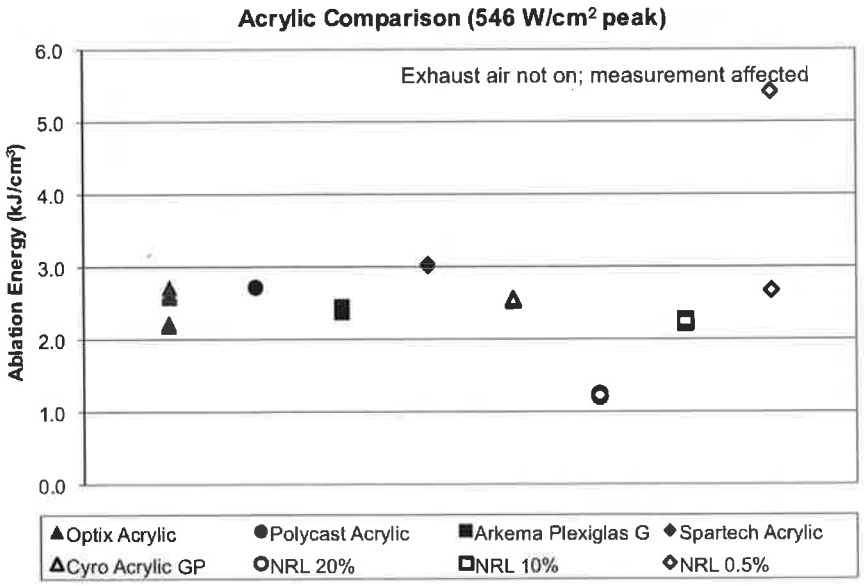


**Fig. 8.** Ablation energies of various commercial acrylic polymers and those synthesized in the lab.

amount of less thermally stable, branched-chain ends in the cross-linked sample. Random bond breaking, resulting in large and small fragments, occurred; thus, a nonuniform ablation was observed. In addition, upon viewing the videos of the ablation process, it was noted that the amount of material fragmentation increased with an increase in the percentage of cross-linking agent added to the PMMA.

### 4.2. Ablation of various acrylic polymers

Cross-linked PMMA samples that were synthesized and previously irradiated were labeled as PMMA due to the generic nature of the material. Upon researching commercially available carbon black–loaded polymers, it was noted that there were several types of PMMA-designated plastics, most of which were referred to simply as "acrylic" plastics. Acrylic is a general term for PMMA that is loosely used by vendors and distributors. Many acrylics are sold with various colorings or toughening fillers for a variety of applications; others are molded in different fashions affording higher or lower molecular weight chains, which can affect ablation rates and energies. Different acrylic variations were acquired and tested to identify a suitable polymer for laser beam profiling and diagnostic measurements. Simple acrylic polymers have proven to be very useful for visualizing laser beam profiles, so finding a representative simple acrylic polymer was necessary not only for beam profiling purposes but for understanding the basic mechanism of degradation as well. Ablation energies of various types of acrylic at 546 W/cm$^2$ (peak) were calculated and can be seen in Fig. 8. Error bars were very small and are not shown due to high reproducibility in the data sets.

Ablation energies for the various acrylics tested were similar, yet whereas some ablated cleanly, others melted or generated a flaky residue upon irradiation. These acrylics were

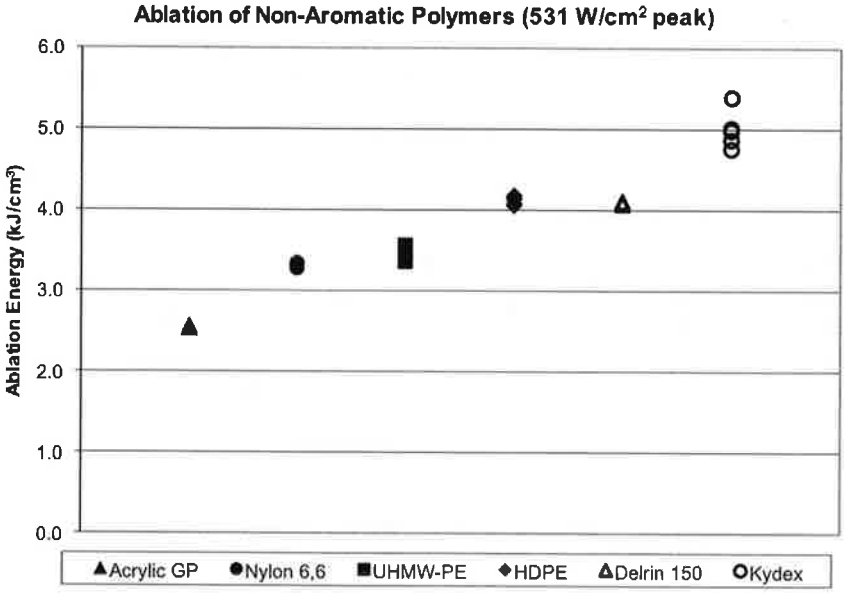


**Fig. 9.** Ablation energies for a series of linear, nonaromatic polymers.

found to contain certain copolymers or mechanical toughening agents, altering their pure acrylic nature. Although their overall thermal stabilities and ablation energies were similar, the degradation mechanisms were not, mostly attributed to these chemical differences and additives. Three synthesized acrylics (PMMA) of various cross-link percentages, labeled NRL (for Naval Research Laboratory), 20%, 10%, and 0.5% by weight, were included to better understand how cross-linked samples compare to commercial acrylics. The nature of polymerization of the synthesized acrylics afforded more branching, and thus less thermal stability, than commercial acrylics when more efficient, bulk polymerization techniques are used to control excessive branching in the polymer. Ablation energies for the synthesized acrylics became similar to those of commercial acrylics as the cross-linking percentage was decreased. The outlying data point (NRL 0.5%) in Fig. 8 was due to the absence of clearing exhaust. Ablation energy averaged ~2.5 kJ/cm$^3$ for the various acrylic samples. Visually some were more cleanly ablated than others.

### 4.3. Ablation of linear, nonaromatic polymers

Several different carbon black–loaded, commercial polymeric materials were irradiated at 1.07 $\mu$m. Nonaromatic polymers included Kydex®, Delrin® 150, Nylon 6,6 (a polyamide), UHMW-PE, HDPE, and a generic acrylic (Acrylite GP). Kydex® is an acrylic/poly(vinyl chloride) (PVC) copolymer; carbon black–loaded PVC was desired for comparison, yet was not commercially available. Delrin® 150 is the trade name given for poly(oxymethylene).

Average irradiance was 500 W/cm$^2$, and peak irradiances were either 531 or 546 W/cm$^2$. Peak irradiance was used to calculate ablation energy due to low thermal conductivity of polymers. Acrylic polymers depolymerize or unzip upon irradiation (heating), giving them lower ablation energy (~2.5 kJ/cm$^3$), as shown in Fig. 9. Because these polymers

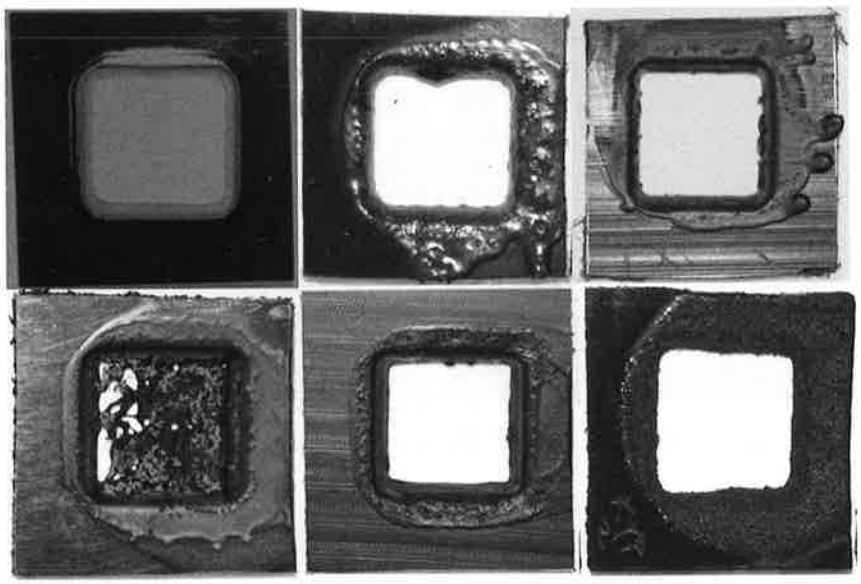

**Fig. 10.** Postirradiation pictures of nonaromatic polymers; from top left: acrylic, Nylon 6,6, UHMW-PE, HDPE, Delrin® 150, and Kydex®.

are ablated as monomer vapor, no fragments or residue is left, and they are referred to as clean ablators. The ablation energy for the polyamide, Nylon 6,6, was ~3.3 kJ/cm$^3$, and melting and bubbling was observed. Postirradiation pictures of the nonaromatic polymers are shown in Fig. 10.

UHMW-PE had an ablation energy of 3.5 kJ/cm$^3$, just slightly higher than that of Nylon 6,6, yet lower than HDPE, which was about 4.1 kJ/cm$^3$. The difference in ablation energy for HDPE and UHMW-PE was attributed to the higher crystallinity (or uniformity in molecular arrangement) in HDPE then in UHMW-PE. The density of HDPE was 0.953 g/cm$^3$, and the density of UHMW-PE was 0.928 g/cm$^3$, a difference of ~3%. UHMW-PE has much higher molecular weight yet is not as crystalline as HDPE; thus, the more crystalline, the harder the material is to ablate. The ablation energy of Delrin® 150, another clean ablator, was very similar to that of HDPE, ~4.1 kJ/cm$^3$.

Kydex®, a copolymer of acrylic and PVC, had the highest ablation energy, averaging ~5.0 kJ/cm$^3$. It is believed that the chlorine heteroatom may increase ablation energy. The electronegativity of heteroatoms such as chlorine plays a role in increasing ablation energy due to attractive interactions between polymer chains. Polymers containing heteroatoms such as bromine and chlorine are typically added as fire retardants, thus promoting charring, which increases ablation energy. Carbon black–loaded PVC was not commercially available for comparison with the copolymer Kydex® material. Its ablation energy is expected to be slightly higher.

Penetration times of the polymer samples were used to calculate ablation energies, and the depth of burn measurements without penetration was determined on at least one of each of the samples to obtain beam profiles. It was determined that two of the ablated polymers could effectively serve as beam profiling materials (i.e., witness plates). Even with penetration, little residual material remained around the edges of the beam spot with

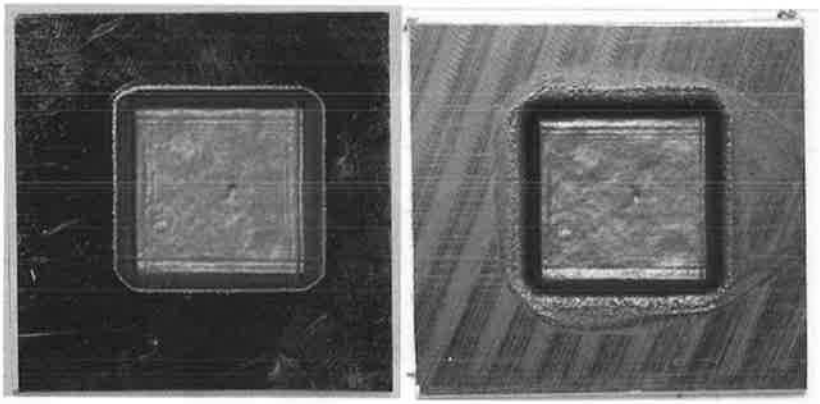

**Fig. 11.** Acrylite GP (left) and Delrin® 150 (right) as quality laser beam profile material.

these materials. Using shorter irradiation times (1 s for Acrylite GP; 2 s for Delrin® 150), beam profiles were obtained for the two polymers. Acrylite GP and Delrin® 150 afforded very precise beam profiles (Fig. 11). There was some residue around the edges of the irradiated spot with Delrin® 150, yet the polymer itself ablated cleanly. Intricate details such as the interference fringes from the beam and peaks, or hot spots, in the beam were clearly visible. The two polymers have simple linear, molecular structure, which upon irradiation vaporizes to leave behind a clean laser footprint. Such polymeric materials are ideal candidates for laser beam diagnostic measurements.

### 4.4. Ablation of PMMA with various carbon black concentrations

The concentration of carbon black in a polymer plays a large role in determining ablation energy at near-IR wavelengths. Particle size and uniformity of dispersion control near-IR laser absorption. Synthesized, non-cross-linked PMMA samples were loaded with various amounts of carbon black to better understand the role carbon black has on ablation. Careful consideration was taken to compensate for nonuniform distribution of carbon black particles. The carbon black was in the form of a functionalized carbon black paste, E80-B (Aerospace Composites, Inc.). Thermogravimetric analysis was performed on the paste to determine the percentage of carbon present after removing the organic component. It was concluded that the paste consisted of ~25% carbon black. This percentage was necessary for calculating the molarity (mol/L) of carbon black in each PMMA sample prepared.

PMMA was formulated containing various concentrations of carbon black. Concentrations of carbon black paste used for loading were on the order of 0.01%, 0.05%, 0.1%, 0.35%, 0.5%, and 1% by weight. These amounts were converted into molarity of carbon black. Peak irradiance was held constant at 517 W/cm$^2$ with a beam spot of ~6.5 cm$^2$. Figure 12 shows ablation energy as a function of carbon black concentration in molarity (calculated from percentage of carbon paste added to polymer). A 90% confidence interval was calculated for average ablation energy. It was concluded that there is no statistical difference in ablation energy where the bars overlap. The percentage of carbon black added to the PMMA, by weight, is shown below the data points.

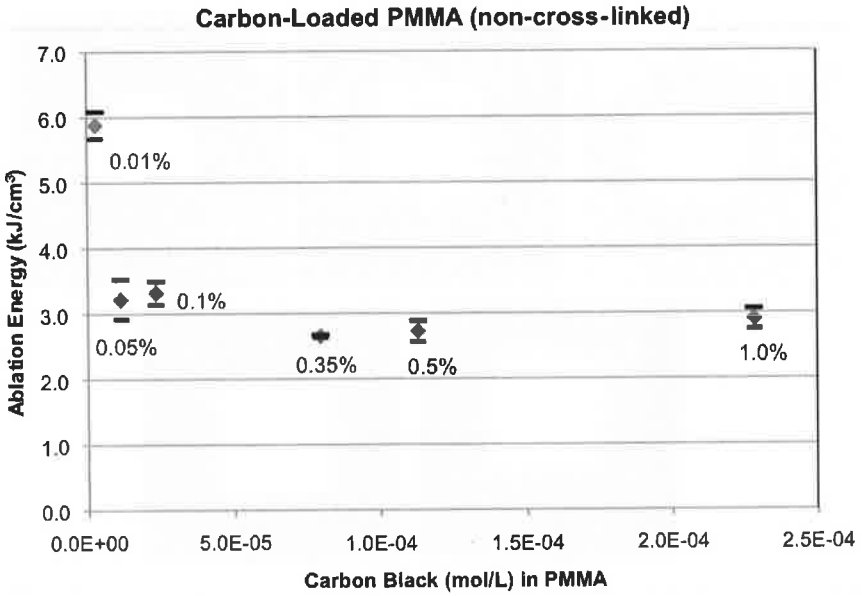


**Fig. 12.** Effect of carbon black concentration on ablation energy in PMMA. Note: Percentages are carbon black paste concentrations added to PMMA by weight; upper and lower confidence intervals included.

It was expected that at lower carbon black concentrations, ablation energy would be higher due to lack of absorption. Much of the laser would be transmitted through the sample at lower concentrations of carbon black; this will be discussed later. Error in the data was attributed to nonuniformity in distribution of carbon black particles from lot to lot. The radical polymerization process used to make the PMMA samples generated high temperatures, increasing the polymerization rate, and some agglomeration of carbon black particles likely occurred. Nonuniformity in dispersion and particle size afforded accounted for the randomness in absorption. However, the figure gives insight on a carbon black concentration threshold for efficient ablation. Postirradiation pictures of PMMA with various concentrations of carbon are shown in Fig. 13. It was concluded that PMMA was more cleanly ablated at carbon black concentrations of $\sim 5.0 \times 10^{-5}$ mol/L (>0.1%). Greater residual material due to adjacent heating of the sample was obvious at lower carbon black concentrations, and thus surface absorption was much smaller.

Ablation energy was $\sim 2.5$ kJ/cm$^3$ in previous tests with commercial and synthesized acrylic samples (with low carbon black content). As shown in Fig. 12, ablation energy likewise reaches a minimum equilibrium value of $\sim 2.5$ kJ/cm$^3$. A good estimate of how much carbon black is actually necessary to achieve this ablation energy threshold can be determined from the graph. The minimum carbon black concentration to obtain this threshold is $\sim 5.0 \times 10^{-5}$ mol/L. Ablation energy rapidly rises with less carbon black added, as absorption tends to zero and more energy is transmitted through the sample.

When compared to PMMA ablation at other wavelengths (e.g., 10.6 $\mu$m), where energy is strongly absorbed near the surface and ablation energies range anywhere from 2.8 to 3.5 kJ/cm$^3$, ablation energies at 1.07 $\mu$m are slightly lower. As more carbon black is incorporated into a polymer, the more of a surface absorber it becomes, thus behaving

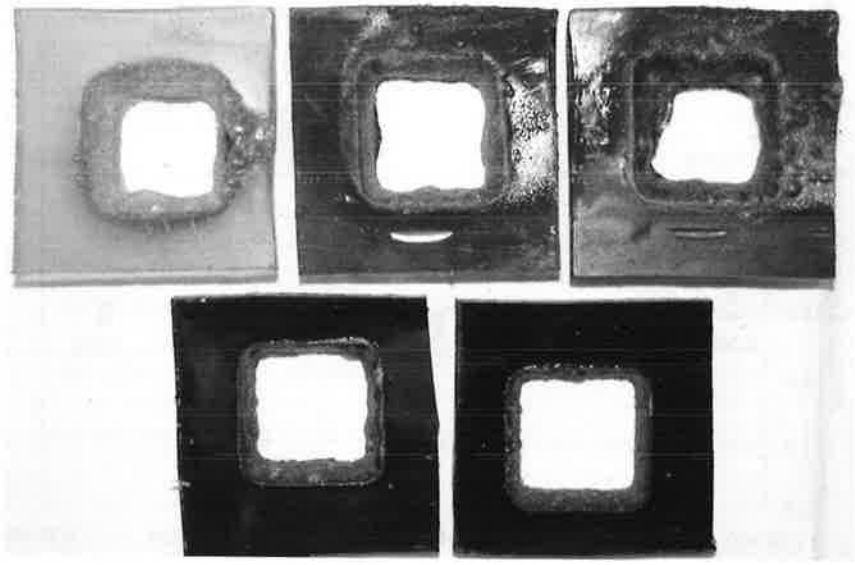

**Fig. 13.** Postirradiation pictures of PMMA with various concentrations of carbon: 0.01%, 0.05%, 0.1%, 0.35%, and 0.5% (listed as percentage of carbon paste added; 1% not shown).

much like PMMA irradiated at 10.6 $\mu$m. This comparison further reinforces the conclusion that in the near-IR as in the IR region, photothermal and not photochemical processes are largely responsible for polymer ablation.

Laser absorption by carbon black plays a significant role in the ablation of PMMA samples. Transmission measurements were made at 1.07 $\mu$m with the power adjusted so as not to damage the sample. This allowed for measurements to be made at the exact wavelength used to ablate the samples. Average transmission values over the beam spot (6.5 $cm^2$) were recorded. The relationship between ablation energy and absorptivity is shown in Fig. 14. The trend is similar to that observed in Fig. 12 in that as absorptivity increases, ablation energy reaches equilibrium around 2.5 $kJ/cm^3$, whereas it tends upward at lower absorptivity.

Figure 15 shows the relationship between absorptivity and carbon black concentration in PMMA. As expected, the data tended to follow a linear trend. At higher concentrations, absorptivity leveled off, possibly due to particle aggregation. Additional data are required to understand this particle concentration effect.

## 5. Effect of Irradiance on Polymers

Studies were also conducted to investigate the effect of irradiance. Four polymer samples were selected: Acrylite GP and FF, Delrin® 150, and PC. Penetration times were recorded, and peak irradiances were used to calculate ablation energy (258, 517, 775 and 1,033 $W/cm^2$). The two Acrylite samples were 1.3 cm thick, whereas the Delrin® 150 and PC were 0.64 cm thick. As shown in Fig. 16, there are data for only two of the four polymeric materials. Acrylite GP and PC were not penetrated even at high irradiance, 1,033 $W/cm^2$, and long irradiation time, 30 s. The aromatic PC samples generated a large amount of char upon irradiation, which prevented penetration.

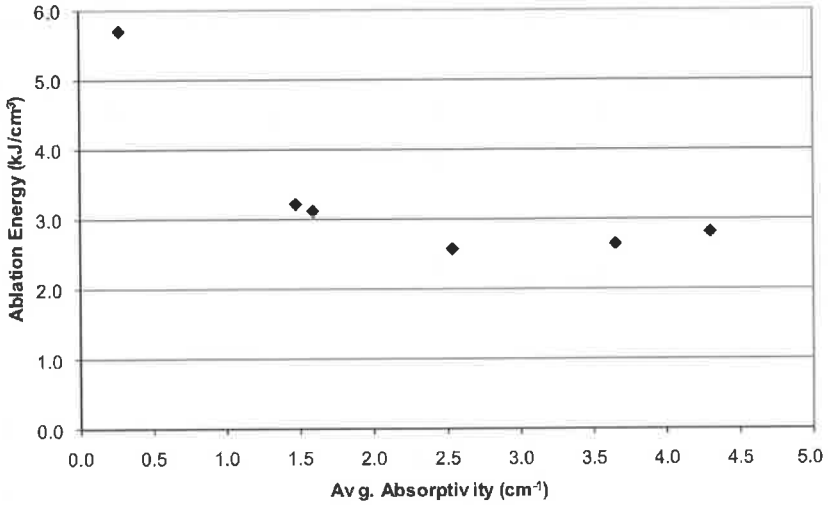


**Fig. 14.** Relationship between ablation energy and absorptivity for carbon-loaded PMMA (averaged values).

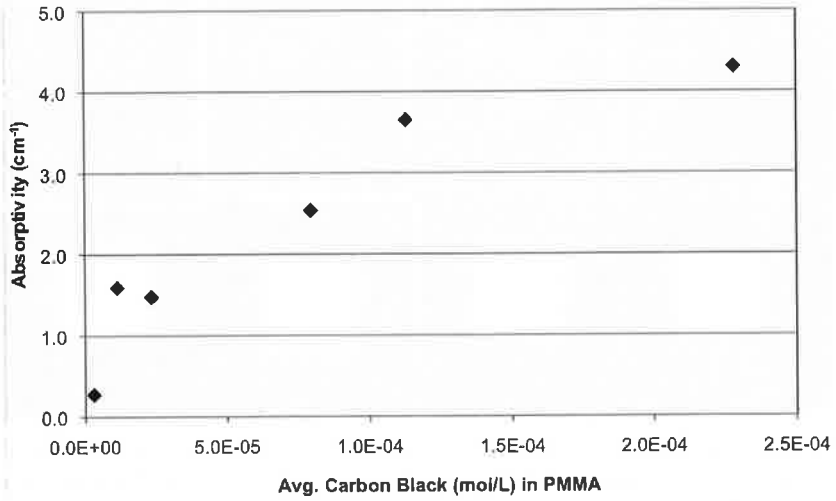


**Fig. 15.** Relationship between absorptivity and carbon black concentration in PMMA (averaged values).

It was unexpected to discover that the 1.3-cm-thick Acrylite GP samples could not be penetrated at 1,033 W/cm$^2$ (and long irradiation times), when 0.64-cm-thick samples were successfully penetrated in previous tests at 531 W/cm$^2$. The postirradiation pictures in Fig. 17 compare Acrylite GP and Acrylite FF samples at different irradiances. The Acrylite FF ablated very cleanly, whereas the Acrylite GP tended to bubble and melt due to in-depth heating and gas formation. After correcting for on-target irradiance, it was believed that the thicker Acrylite GP samples may not be pigmented with carbon black but rather a dye that is a poor absorber in the near-IR.

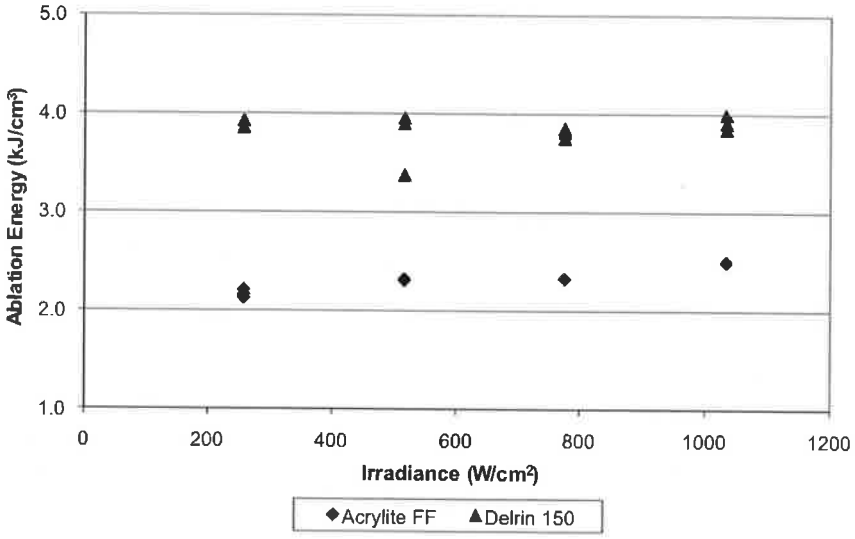


**Fig. 16.** Ablation energy versus irradiance for Acrylite FF and Delrin® 150.

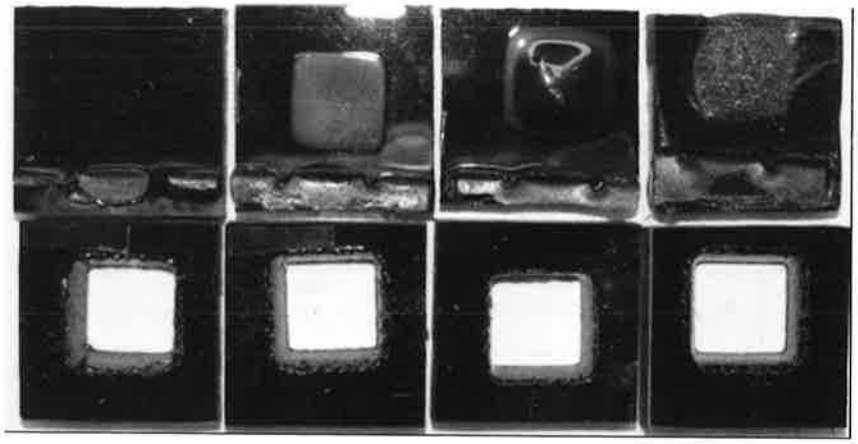

**Fig. 17.** Irradiation of Acrylite GP colored with dye (top) vs. Acrylite FF colored with carbon black pigment (bottom). Irradiances of 258, 517, 775, and 1,033 W/cm$^2$ were used (from left to right).

To confirm the composition of the pigment in the samples, pieces of 0.64-cm-thick Acrylite GP and 1.3-cm-thick Acrylite GP and FF were dissolved in solvent, and near-IR and UV–vis absorbance measurements were made. The spectra in Fig. 18 show the relative near-IR absorbance between 900 and 2,500 nm for each of the three samples. Relative absorbance was used to take into account the concentration of each sample dissolved in solvent. The laser wavelength of interest (1.07 $\mu$m) is identified by the vertical line in the graph. Before analyzing the spectra, it was observed that the dissolved solution of 1.3-cm-thick Acrylite GP was greenish, whereas the thinner GP sample and the Acrylite FF sample were black. It was believed that the pigment in the thick Acrylite GP sample was in fact

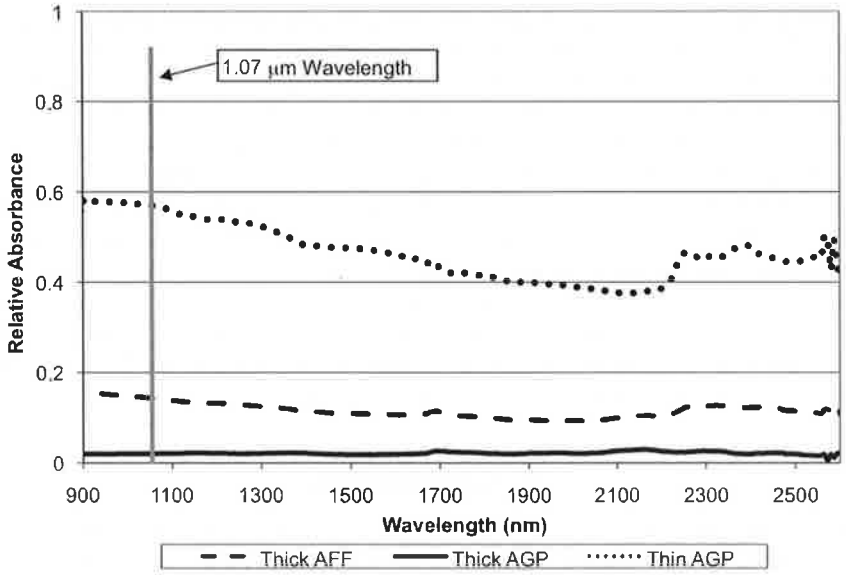


**Fig. 18.** Near-IR spectra of Acrylite samples containing carbon black pigment and dye.

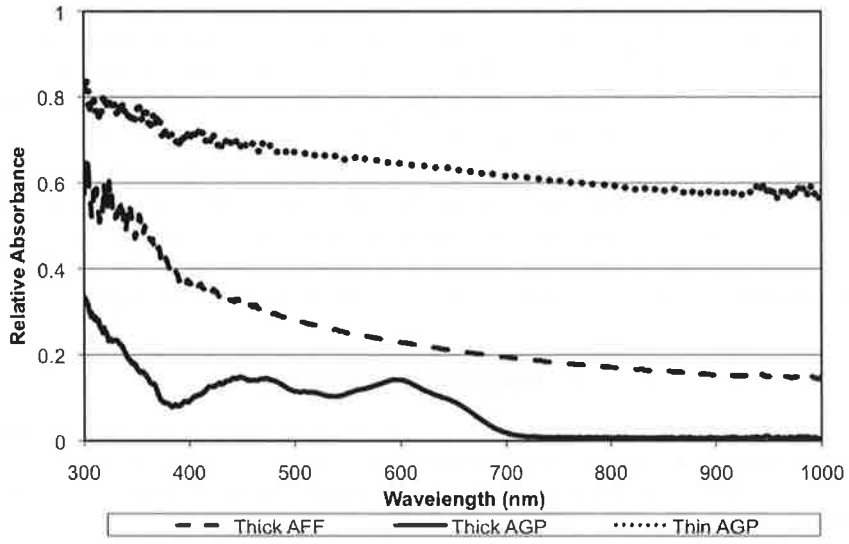


**Fig. 19.** UV–vis spectra of Acrylite samples containing carbon black pigment and dye.

a dye. The low absorbance measurement indicated further that it was likely a dye and not carbon black. The samples with carbon black pigment showed considerably more absorbance. Not only did the near-IR spectra show the presence of a dye in one of the three samples, but it also helped to explain the difference in ablation energy that was observed between the two carbon black–loaded samples, thin Acrylite GP and thick Acrylite FF.

When the UV–vis spectra of each sample were taken, the absorbing dye was identifiable in the 400–800-nm wavelength range, typical for organic dyes (Fig. 19). It should be noted that the small dip in the spectrum of the dye-containing Acrylite GP sample at ~540 nm is

in the green region of the visible spectrum: thus, the greenish color of dissolved polymer solution that was observed. Two peaks at ~450 and 600 nm correspond to two different unknown dyes; a two-dye pigment system is commonly used to give polymers a dark, seemingly black color. The need for a carbon black–based versus a dye-based polymeric material, regarding the calculation of polymer ablation energies and laser beam profile diagnostics purposes at 1 $\mu$m, was clearly identified as a result. The dye-based Acrylite polymer absorbed much less than the carbon black–based Acrylite polymers. Using Beer's law and the absorbance measurements at 1.07 $\mu$m obtained from the near-IR spectra in Fig. 18, the amount of laser energy absorbed at some thickness in the polymer samples was determined. Upon calculation, it was concluded that the thin Acrylite GP sample was absorbing >99% of the energy at a depth of 0.1 cm in the sample. The thicker Acrylite FF sample absorbed ~93% of the energy at the same depth, whereas the thick Acrylite GP sample (dye-based) absorbed only ~5% of the energy at 0.1 cm.

## 6. Conclusions

Ablation energies for several laboratory-synthesized and commercial polymers were measured in the near-IR. Results were found to be dependent on the molecular structure of the polymer, especially the aromatic and heteroatomic character, and the nature of the thermal degradation processes. Linear, nonaromatic polymers such as acrylic and high-density polyethylene unzip or depolymerize without charring and generally have low ablation energies on the order of 2–4 kJ/cm$^3$. Cross-linked or in-chain aromatic polymers containing oxygen generally form $CO_2$ and residual carbonaceous char upon irradiation, resulting in increased black body reradiation and higher ablation energy. Two ideal polymers for irradiance diagnostics, Acrylite FF and Delrin® 150, were identified as quality materials for laser beam profile and diagnostic purposes. In addition, polymeric materials that are colored with dyes rather than pigments are poor absorbers in the near-IR, and polymer damage is minimal compared to carbon black–loaded polymers. The study was aimed at understanding the role of molecular structure on polymer ablation in the near-IR and to identify polymeric materials suitable for detailed laser beam profiling purposes.

## 7. Acknowledgments

The authors would like to acknowledge the support from Naval Sea Systems Command, PMS-405, Directed Energy and Electric Weapon Systems Program Office, the Directed Energy Technology Office (DETO) at the Naval Surface Warfare Center, Dahlgren, and the Electro-Optics Center/Pennsylvania State University. The authors would also like to thank the Naval Research Laboratory Chemistry Division and Edison Memorial Graduate Training Program for support and funding.

## References

[1]Blanchet, G. B., Macromolecules **28**, 4603 (1995).
[2]Blanchet, G. B., Journal of Applied Physics **80**, 4082 (1996).
[3]Blanchet, G. B., and C. R. Fincher, Applied Physics Letters **65**, 1311 (1994).
[4]Costela, A., J. M. Figuera, F. Florido, I. Garciamoreno, E. P. Collar, and R. Sastre, Applied Physics A—Materials Science & Processing **60**, 261 (1995).
[5]Cozzens, R. F., and R. B. Fox, Polymer Engineering and Science **18**, 900 (1978).

[6]Cozzens, R. F., P. Walter, and A. W. Snow, Journal of Applied Polymer Science **34**, 601 (1987).
[7]Garrison, B. J., and R. Srinivasan, Journal of Vacuum Science & Technology A—Vacuum Surfaces and Films **3**, 746 (1985).
[8]Garrison, B. J., and R. Srinivasan, Journal of Applied Physics **57**, 2909 (1985).
[9]Joeckle, R., B. Gautier, F. Lacroix, S. Clemens, and L. T. My, SPIE Proceedings: Gas Flow and Chemical Lasers **1810**, 624 (1992).
[10]Joeckle, R., A. Koneke, and A. Sontag, SPIE Proceedings: Gas Flow and Chemical Lasers **1397**, 679 (1990).
[11]Joeckle, R., G. Rapp, and A. Sontag, SPIE Proceedings: Gas Flow and Chemical Lasers **1397**, 683 (1990).
[12]Kawamura, Y., K. Toyoda, and S. Namba, Applied Physics Letters **40**, 374 (1982).
[13]Said-Galiev, E. E., and L. N. Nikitin, Mechanics of Composite Materials **28**, 97 (1992).
[14]Srinivasan, R., Journal of Applied Physics **70**, 7588 (1991).
[15]Srinivasan, R., Journal of Applied Physics **73**, 2743 (1993).
[16]Srinivasan, R., and B. Braren, Journal of Polymer Science Part A—Polymer Chemistry **22**, 2601 (1984).
[17]Srinivasan, R., and V. Mayne-Banton, Applied Physics Letters **41**, 576 (1982).

## The Authors

**Mr. Collin J. Bright** received his Bachelor's degree in 2007 from Elon University. He is currently employed by SAIC as a chemist at the Naval Research Laboratory, where he is involved with HEL/materials interactions and nonlinear optical materials for protection from and detection of potentially damaging lasers.

**Dr. Robert F. Cozzens** received a B.S. in chemistry in 1963 and a Ph.D. in 1966 from the University of Virginia. He is a Professor of Chemistry at George Mason University in Fairfax, Virginia, and a Senior Research Scientist (Intermittent) at the Naval Research Laboratory in Washington, D.C. Dr. Cozzens has been involved for more than 30 years in the interaction of laser radiation with materials, including polymeric composites, metals, and sensors. He has published and presented numerous research papers and technical reports and periodically has served as consultant and expert witness with law firms. He is also a member of several professional societies.

**Mr. Peter D. Kazunas** is a senior at Indiana University of Pennsylvania, where he majors in applied physics/electro-optics. His concentrations include remote sensing, numerical methods, and LADAR. He has worked as an intern at the Penn State Electro-Optics Center for 3 years in the High Energy Laser Effects Lab, where he has gained experience in testing beam interaction with materials, beam diagnostics, and beam combining.

**Dr. Christopher T. Lloyd** received his Master's degree in chemistry in 2003 and his Ph.D. in physical sciences from George Mason University in January 2009. He is currently employed as a research chemist at NSWC–Dahlgren in the materials lethality group. He worked at the Naval Research Laboratory for more than 8 years studying HEL/materials interactions and applied polymer science. His work involves such tasks as identifying unknown materials and composites and retroengineering samples for laser lethality measurements. Dr. Lloyd has published and presented research involving the synthesis of organic molecules and the effects of high-energy lasers on organic matrix composites at numerous national meetings and symposia.

**Mr. Larry K. Myers** joined the EOC in 2004 as a Senior Engineering Aide running the High Energy Effects Laboratory. He is responsible for laboratory operations, including optical and diagnostic system configuration and conducting experiments. He has contributed to several successful laser programs from inception through execution. Prior to the EOC, Larry was a Junior Electronics Engineer at Biocontrol Technology, Inc., developing hardware for a noninvasive glucometer.

**Mr. D. Jason (Jake) Sames** received his Bachelor's and Master's degrees in engineering science from Penn State University studying novel applications of laser-induced breakdown spectroscopy. Mr. Sames has experience in a wide array of laser applications, ranging from spectroscopy, to surface coating removal, to optical characterization of fiber-optic components for telecommunications. Since 2002, he has been employed at the Penn State Electro-Optics Center, actively involved in HEL weapons–related research. Currently, he is a Principal Investigator at EOC in partnership with the NSWC–Dahlgren in-coherent beam combining programs "Laser Weapon System," or "LaWS."